

AD-R139 453

A STUDY ON THE PREDICTION OF THE STARTING TRANSIENT
PROCESS OF SOLID PROP. (U) FOREIGN TECHNOLOGY DIV
WRIGHT-PATTERSON AFB OH T C CHIEN ET AL. 22 FEB 84
FTD-ID(RS)T-0069-84

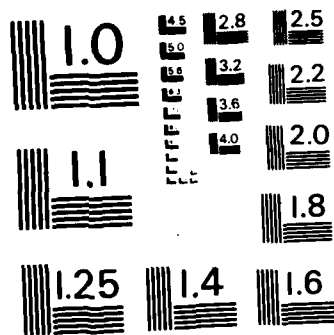
1/1

UNCLASSIFIED

F/G 21/2

NL





MICROCOPY RESOLUTION TEST CHART
NATIONAL BUREAU OF STANDARDS-1963-A

2

FTD-ID(RS)T-0069-84

AD A139453

FOREIGN TECHNOLOGY DIVISION



A STUDY ON THE PREDICTION OF THE STARTING TRANSIENT PROCESS
OF SOLID PROPELLANT ROCKET MOTORS

by

C. Tse-ch'un, H. Hung-Ch'ing



DTIC
ELECTE
MAR 28 1984
S **D**
B

Approved for public release;
distribution unlimited.

DTIC FILE COPY

84 03 27 683

EDITED TRANSLATION

FTD-ID(RS)T-0069-84

22 February 1984

MICROFICHE NR: FTD-84-C-000212

A STUDY ON THE PREDICTION OF THE STARTING TRANSIENT
PROCESS OF SOLID PROPELLANT ROCKET MOTORS

By: C. Tse-ch'un, H. Hung-Ch'ing

English pages: 13

Source: Yuhang Xuebao, Nr. 4, 1982, pp. 44-51

Country of origin: China

Translated by: SCITRAN

F33657-81-D-0263

Requester: FTD/SDBP

Approved for public release; distribution unlimited.

THIS TRANSLATION IS A RENDITION OF THE ORIGINAL FOREIGN TEXT WITHOUT ANY ANALYTICAL OR EDITORIAL COMMENT. STATEMENTS OR THEORIES ADVOCATED OR IMPLIED ARE THOSE OF THE SOURCE AND DO NOT NECESSARILY REFLECT THE POSITION OR OPINION OF THE FOREIGN TECHNOLOGY DIVISION.

PREPARED BY:

TRANSLATION DIVISION
FOREIGN TECHNOLOGY DIVISION
WP-AFB, OHIO.

GRAPHICS DISCLAIMER

All figures, graphics, tables, equations, etc. merged into this translation were extracted from the best quality copy available.



| | |
|--------------------|-------------------------------------|
| Accession For | |
| NTIS GRA&I | <input checked="" type="checkbox"/> |
| DTIC TAB | <input type="checkbox"/> |
| Unannounced | <input type="checkbox"/> |
| Justification | |
| By _____ | |
| Distribution/ | |
| Availability Codes | |
| Dist | Avail and/or Special |
| A-1 | |

A STUDY ON THE PREDICTION OF THE STARTING TRANSIENT PROCESS OF SOLID PROPELLANT ROCKET MOTORS

Chien Tse-ch'un, Ho Hung-Ch'ing

ABSTRACT

The interior ballistic $P(x, t)$ model of the starting transient process of the solid propellant rocket motor has been improved in the present paper, with the aim of ensuring better accordance with the actual working conditions in the motor. The numerical solution of the governing equations, pertaining to one-dimensional unsteady gas dynamics, utilizes an implicit finite-difference scheme combined with the method of characteristics. The computed pressure-time curve is in fair agreement with the experimentally measured one. It is evident from the results of computation that erosive burning is a main factor affecting the starting pressure-peak for a given propellant geometry, and the heat exchange between the combustion-gas and the solid propellant casts a great influence upon the processes of ignition-induction and flame-spreading. Moreover the rate of pressure change also plays an important role in the phases of flame-spreading and chamber-filling, and should hence be accounted for in the prediction. The computation program presented should provide a general means for accurate prediction of the interior ballistic curve of starting transient process, as well as for the investigation of the influences on it of the various factors involved.

I. Introduction

The interior ballistic curve of a solid propellant rocket consists of the starting transient stage, the operating stage and the trailing stage (Figure 1). The starting transient stage, in turn, is made up of the ignition-induction stage, the flame-spreading stage and the chamber-filling stage. Ignition delay, rate of pressure increase and peak value of the initial pressure may be determined through computation of the starting process. The purpose of in-depth studies of the starting transient process is: 1. to obtain an accurate prediction method of the starting transient process to serve as a basis for the choice by the designer of appropriate propellant geometry, initial combustion surface and shell body thickness, thus raising as much as possible

This paper was received on April 26, 1982.

the mass ratio of the motor, reducing the number of necessary ground tests, and thus slashing cost and shortening the period of fabrication. 2. to study the effect of various parameters so as to provide a basis for the control of the starting transient process.

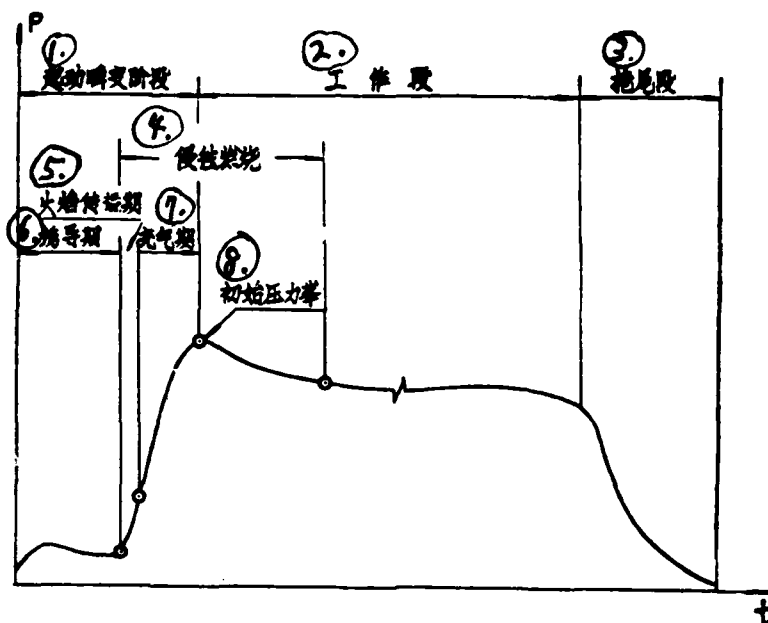


Figure 1. Schematic diagram of the operation of a solid propellant rocket motor. 1--starting transient stage; 2--operating stage; 3--trailing stage; 4--erosive burning; 5--flame-spreading stage; 6--ignition-induction stage; 7--chamber-filling stage; 8--peak of initial pressure

/45

Two models were adopted abroad in the 60's for the study of the starting transient process. The first is a constant, steady, one-dimensional flow model (the $p(x)$ model) which assumes that the combustion gas parameters, p , T and u , vary only with the axial position at a given instant of time. The second model assumes that p , T and u do not vary along the passage, but only vary with time (the $p(t)$ model). In the 70's, Kuo, K. K., first took into consideration both the space and time dependence of these parameters (the $p(x,t)$ model) in the solution of the one-dimensional unsteady gas dynamics equations, and accomplished the computation of the starting transient process of granular propellants [1]. Later,

this model was generalized by Pertz, et al., [2] and applied to solid propellant rocket motors. As the $p(x,t)$ model can be used to compute simultaneously the variation with time and space of the combustion gas parameters, it gives a more nearly true reflection of the transient processes of ignition-induction, flame-spreading and combustion chamber-filling. Moreover, in contrast with the $p(t)$ model, the $p(x,t)$ model allows the cross-sectional area of the solid propellant passage to vary along the axial direction.

Up until today, on the $p(x)$ model and the $p(t)$ model have been used in this country. To better understand the starting transient 1,2 process, we have improved the $p(x,t)$ model, written a FORTRAN program, and given the computed results for the cases where certain parameters have been changed.

Notations

| | |
|-----------------|---|
| A_b | combustion surface, cm^2 |
| A_p | cross-sectional area of passage, cm^2 |
| A_t | area at the throat of the engine nozzle, cm^2 |
| a | coefficient of combustion rate in the formula for combustion rate $r = ap^n$ |
| b | combustion perimeter, cm |
| h_c | local convection heat exchange coefficient, $\text{kcal}/\text{cm}^2 \cdot \text{sec} \cdot \text{k}$ |
| I_u, I_p, I_T | inhomogeneous terms of the governing equations, Eq. (1) |
| J_C | mechanical equivalent of heat, $0.4267 \times 10^5 \text{ kg} \cdot \text{cm}/\text{kcal}$ |
| \dot{m}_{ig} | igniter gas mass flow rate, $\text{kg} \cdot \text{sec}/\text{cm}$ |
| n | pressure index |
| p | static pressure, kg/cm^2 |
| p_1 | pressure at the bow, kg/cm^2 |
| q_1 | heat flow rate, $\text{kcal}/\text{cm}^2 \cdot \text{sec}$ |
| R | gas constant of the combustion gas, $\text{kg} \cdot \text{cm}/\text{kg} \cdot \text{k}$ |
| r | combustion rate of solid propellant, cm/sec |
| r_0 | steady-state combustion rate, cm/sec |
| T | static temperature of the combustion gas, K |

| | |
|-----------|--|
| T_f | temperature of the adiabatic flame, K |
| T_{pi} | initial temperature of the propellant, K |
| T_{ps} | local surface temperature of the propellant, K |
| T_{sig} | critical ignition temperature of propellant, K |
| t | time, sec |
| u | velocity of gas, cm/sec |
| u_{tv} | limiting velocity of erosive burning, m/sec |
| V_{es} | volume of passage upstream x_o , cm^3 |
| x_o | the axial coordinate of the point first ignited, cm |
| x_p | the axial coordinate of the front section of the solid propellant, cm |
| α | coefficient of heat diffusion, cm^2/sec |
| λ | heat conduction coefficient (in the absence of a subscript, it refers to the gas), kcal/cm \cdot sec \cdot k |
| ρ | density (in the absence of a subscript, it refers to the gas), kg sec 2 cm $^{-4}$ |

Subscripts:

| | |
|----|-----------------|
| e | nozzle entrance |
| es | upstream x_o |
| fr | flame front |
| i | initial value |
| ig | igniter |

II. Physical model

The physical process of the starting transient process can be described as follows:

1. Solid propellant ignition-induction stage

The high temperature combustion gas from the igniter produces changes in the parameters of the flow field in the passage, and undergoes heat exchange with the surface of the solid propellant. When the net energy acquired at a certain location on the propellant surface becomes high enough to maintain spontaneous combustion,

ignition occurs at that location. It is usually thought that the heat flow is greatest where the flame from the igniter comes in contact with the surface of the propellant (Figure 2, x_0), and this is where the propellant becomes ignited first. The position of x_0 may be computed with the help of high speed photography of the shape of the flame from the igniter and knowledge about the propellant geometry. It may also be obtained from measurements of the heat flow in the ignition process.

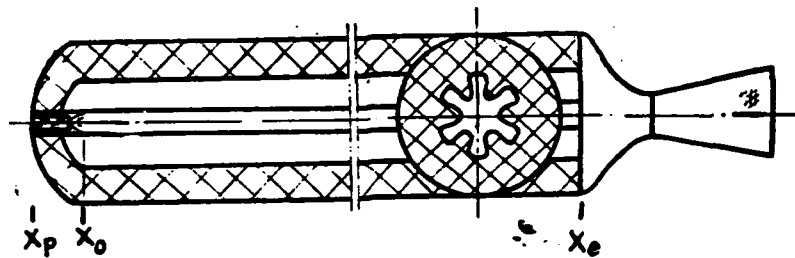


Figure 2. Schematic diagram of a solid propellant rocket motor

2. Flame spreading stage

After the propellant is ignited locally on the surface, the additional increase in mass and energy from the propellant enhances the transfer of energy toward the unignited parts of the surface, causing the surface of the propellant close to the flame tip to be ignited rapidly. Thus, the flame spreads from x_0 upstream and downstream, until the entire surface of the propellant is ignited.

3. Chamber-filling stage

After the entire surface of the propellant is ignited, erosive burning and the instantaneous rate of change in pressure cause the rate of formation of the combustion gas to increase continually. Pressure in the combustion chamber rapidly builds up and an initial pressure peak is produced.

In summary, the physical factors we have taken into consideration include: (1) positioning of the igniter in the propellant passage at the bow of the motor, (2) the heat exchange process and friction between the combustion gas and the combustion surface of the solid propellant, (3) ignition of the propellant with the flame spreading upstream and downstream, (4) the effect of the erosive burning, (5) the effect of the instantaneous rate of change of pressure and (6) the cross-sectional area of the passage being continually variable along the axial direction. Among these, (1), (3) and (6) constitute the improvements we have made in this paper.

In this manner, the physical model considered is a fairly close representation of the actual operating conditions of the motor.

/47

III. Analytical model

1. The governing equations

Take the point x_0 , where the flame from the igniter impinges on the surface of the propellant, and the nozzle entrance x_e to be, respectively, the left and right boundary of the flow field (Figure 2). Assume that: (1) the effect of the solid phase on the flow is neglected; (2) the combustion gas obeys the ideal gas law, and the isobaric specific heat, specific heat ratio, average molecular weight and gas constant are the same for the combustion gases of the igniter and the propellant, and remain constant; (3) combustion of the propellant is limited to the thin layer of gaseous phase close to the surface of the propellant, and the addition of combustion gas to the passage has zero axial velocity component. After listing and transforming the equation of continuity, the momentum conservation equation and the energy conservation equation, we obtain the following set of governing equations for one-dimensional unsteady gas dynamics.

$$\begin{aligned}
\frac{\partial u}{\partial t} + u \frac{\partial u}{\partial x} + g \frac{RT}{p} \frac{\partial p}{\partial x} &= -\frac{\rho_p b g R T}{A_p} \frac{1}{p} u^r - \frac{b}{A_p} f_c \frac{u^2}{2} \equiv I_s \\
\frac{\partial p}{\partial t} + r p \frac{\partial u}{\partial x} + u \frac{\partial p}{\partial x} &= -\frac{r p u}{A_p} \frac{\partial A_p}{\partial x} + (r-1) \left(J_c g C_p T_f + \frac{u^2}{2} \right) \\
&\quad \cdot \frac{\rho_p b}{A_p} r - (r-1) \frac{b}{A_p} \left(J_c q_1 - \frac{1}{2 g R T} p f_c u^2 \right) \equiv I_p \\
\frac{\partial T}{\partial t} + (r-1) T \frac{\partial u}{\partial x} + u \frac{\partial T}{\partial x} &= -(r-1) T \frac{u}{A_p} \frac{\partial A_p}{\partial x} + \frac{T}{p} \frac{b}{A_p} \\
&\quad \cdot \left[r g R \rho_p \left(T_f + \frac{u}{2 J_c C_p g} - \frac{T}{r} \right) r - (r-1) \left(J_c q_1 - \frac{1}{2 g R T} p f_c u^2 \right) \right] \equiv I_T
\end{aligned} \tag{1}$$

The initial conditions are

$$p = p_i, \quad u = u_i, \quad T = T_i \tag{2}$$

Equation (1) is a set of pseudo-linear, inhomogeneous, hyperbolic partial differential equations. Its three characteristic directions and the corresponding compatible equations are, respectively, the characteristic line I along the right side

$$\begin{aligned}
\left[\frac{dx}{dt} \right]_I &= u + C & \left[\frac{dp}{dt} \right]_I &= -\frac{r p}{C} \left[\frac{du}{dt} \right]_I + I_p + \frac{r p}{C} I_s \\
\text{the characteristic line II along the left side} \\
\left[\frac{dx}{dt} \right]_{II} &= u - C & \left[\frac{dp}{dt} \right]_{II} &= \frac{r p}{C} \left[\frac{du}{dt} \right]_{II} + I_p - \frac{r p}{C} I_s \\
\text{the locus line III along the fluid} \\
\left[\frac{dx}{dt} \right]_{III} &= u & \left[\frac{dT}{dt} \right]_{III} &= \frac{\gamma-1}{\gamma} \frac{T}{p} \frac{dp}{dt} + I_T - \frac{\gamma-1}{\gamma} \frac{T}{p} I_p
\end{aligned} \tag{3}$$

The equation for the rate of combustion is taken to be the erosion relation [3] proposed by Kuo, K. K., on the basis of a thermo-chemical model of gas dynamics. We also take into consideration the rapid rise of pressure in the combustion chamber during chamber-filling. Combining the above with the effect of rate of pressure variation dp/dt on the rate of combustion [4], we obtain

$$r = r_s \left[1 + K_1 P^{K_2} (u - u_{cr})^{K_3} + \frac{K_{11} n a p_r}{r_s^2 p} \frac{dp}{dt} \right] \tag{4}$$

The temperature of the surface of the propellant is computed from the following ordinary differential equation:

$$dT_{ps}/dt = 4a_p h_c^2 (T - T_{ps})^2 / [3\lambda_{pr}^2 (T_{ps} - T_{pi})(2T - T_{ps} - T_{pi})] \quad (5)$$

The initial condition is $T_{ps}(x, 0) = T_{pi}$. When $T_{ps} \geq T_{sig}$ on the computed cross-section, the propellant is ignited at that position.

2. Boundary conditions

/48

Take the section $x_p \leq x \leq x_0$ to the left of the left boundary x_0 as the front section (Figure 2). The flow field is rather complex there. Assume that the front section has a uniform distribution of pressure and temperature. Computations have shown that variations in temperature and pressure in the front section are not large. We obtain from the continuity equation and the energy conservation equation applied to the front section

$$\left. \begin{aligned} dp_{x_0}/dt &= \left[\dot{m}_{ig}(t) \gamma g R T_{ig} + r A_{bes} \rho_p \gamma g R T_f \right. \\ &\quad \left. - \gamma p_{x_0} u_{x_0} A_{p_{x_0}} - \frac{(\gamma-1) A_{p_{x_0}}}{2gR T_{x_0}} p_{x_0} u_{x_0}^2 \right] / V_{x_0} \\ dT_{x_0}/dt &= \left[g R T_{x_0} / p_{x_0} \dot{m}_{ig} (\gamma T_{ig} - T_{x_0}) + \frac{A_{bes} r \rho_p r}{p_{x_0}} \right. \\ &\quad \left. - g R T_{x_0} (\gamma T_f - T_{x_0}) - (r-1) A_{p_{x_0}} u_{x_0} \left(T_{x_0} + \frac{u_{x_0}^2}{2gR} \right) \right] / V_{x_0} \end{aligned} \right\} \quad (6)$$

The initial conditions are

$$T_{x_0}(0) = T_i, \quad p_{x_0}(0) = p_i$$

These plus the equations corresponding to the characteristic line along the left side in equation (3) constitute the left boundary conditions. A_{bes} denotes that part of the surface (6) in the front section that is already undergoing combustion. It is found from the distance by which the flame has spread to the left.

The right boundary conditions are formed by taking the equations for the one-dimensional, isentropic, constant steady choked or unchoked (before the nozzle becomes choked) flow of the nozzle, combined with the equations in (3) that correspond to the

characteristic line along the right side and those corresponding to the locus line of the fluid. Before the choke lid is opened, $u_e = 0$.

IV. Numerical solution

An implicit finite-difference scheme is combined with the method of characteristics to solve the partial differential equations whose inhomogeneous terms have been linearized. We finally arrive at a set of linear algebraic equations which enable one to solve for the gas flow parameters at the various nodes at time $j + 1$ given the parameters for the various nodes at the time j .

$$\begin{pmatrix} A_1 & C_1 & & & & \\ B_1 & A_1 & C_1 & & & \\ & \dots & \dots & \dots & & \\ & & B_n & A_n & C_n & \\ & & & \dots & \dots & \\ & & & & B_{m-1} & A_{m-1} \end{pmatrix} \begin{pmatrix} U_1^{j+1} \\ U_2^{j+1} \\ \dots \\ U_n^{j+1} \\ \dots \\ U_{m-1}^{j+1} \end{pmatrix} = \begin{pmatrix} F_1 - B_1 U_1^{j+1} \\ F_1 \\ \dots \\ F_n \\ \dots \\ F_{m-1} - C_{m-1} U_{m-1}^{j+1} \end{pmatrix} \quad (7)$$

In the above, U_0^{j+1} and U_m^{j+1} are, respectively, the combustion gas parameters, u , p and T on the left and right boundary at time $j + 1$, and are solved from the left and right boundary conditions, respectively. A , B and C are 3×3 submatrices, and U and F are 3×1 submatrices.

The left and right boundary conditions have also been transformed into algebraic equations in a similar manner.

Two points need to be mentioned here about the procedure of solving these equations:

1. After the propellant first becomes ignited at x_0 , the flame spreads simultaneously upstream and downstream. One may proceed with the computation as follows. First, assume an acceleration for the spreading of the flame toward the left. Use this to calculate the area A_{bes} of the front section that has already been ignited. Substitute this into the left boundary condition which

then is used along with the right boundary condition to solve the computational equations, Equation (7), for the governing equations. After the acceleration of the spreading of the flame towards the right from point x_0 to a neighboring node downstream has been computed, the process of computation is started anew from the time x_0 is ignited, the acceleration of flame spreading toward the right being used to correct that toward the left. This procedure is repeated until two successive acceleration values obtained for the spreading of flame toward the left are very close to each other.

2. By taking into consideration the increase in rate of combustion due to the rate of change of pressure dp/dt in the combustion rate relation (4), we will amplify any small error in pressure in the computation and cause sharp oscillations in the $p-t$ curve for the flame-spreading stage. This difficulty is overcome by adopting large steplength $\Delta p/\Delta t$ instead of dp/dt , and resorting to the method of iterative correction.

/49

V. Results of computation, analysis and conclusion

The numerical computation was carried out for the G5 motor. See Table 1 for the numerical inputs.

TABLE 1. Numerical inputs

| Geometric parameters of the motor | | Properties of the propellant | | | | Combustion gas parameters | |
|-----------------------------------|--------|------------------------------|-------------------------|-----------|-------------------------|---------------------------|--------|
| x_p | -3.5 | λ_p | 0.1286×10^{-5} | u_{1r} | 63.90 | r | 1.165 |
| x_0 | 10.0 | C_{pr} | 0.29 | K_{11} | 0.5 | W | 27.30 |
| x_r | 125.7 | δ_p | 1.8×10^{-3} | K_2 | 0.2144×10^{-2} | R | 3100.0 |
| A_1 | 50.72 | σ_p | 0.0023 | K_p | 0.35 | C_p | 0.5023 |
| V_{e11} | 1391.6 | T_{ref} | 293.0 | K_u | 0.69 | P_r | 0.8847 |
| $b_1(x)$ | 81.84 | α | 0.2106 | T_{110} | 560.0 | T_{100} | 2250.0 |
| $A_{p1}(x)$ | 113.54 | n | 0.3863 | e_r | 0.01 | | |

In the computations, we have used different values for the initial values, the adiabatic flame temperature of the propellant, the mass flow rate for the igniter, erosive combustion rate, heat exchange coefficient and ignition temperature of the propellant.

All the computations are steady and convergent. The results of these computations, analysis and conclusions arrived at are presented below.

1. Figure 3 gives the p-t curve for the starting transient process. It can be seen that the curve that takes into account the effect of dp/dt is closer to the experimental curve for the G5 motor. Therefore, the computational procedure presented in this paper can be used to accurately predict the starting transient process, and to study the effects of the various factors involved.

In addition, the curve also exhibits the phenomenon of spontaneous acceleration of flame-spreading.

2. It can be seen from Figures 3 and 4 that dp/dt has a marked effect on the p-t curve and the gas flow parameters, and should, therefore, be properly taken account of. It can be seen that, owing to the effect of the instantaneous changes in the pressure, the velocity of flame-spreading is increased, the rate of pressure increase is raised, the time required to reach the initial pressure peak is shortened, and the combustion gas velocity at every point of the flow field is increased. This is because when the pressure increases sharply, the combustion rate of the propellant is increased, the rate of mass flow is increased, and the effect of erosive burning is enhanced.

3. The erosive property of the propellant has a large effect on the initial pressure peak value as well as the rate of pressure increase (Figure 5). In the study of the parameters, it was found that for a given geometry of the propellant, erosive burning is the major factor affecting the initial pressure peak value.

4. Figure 6 reflects the strong influence of the heat exchange between the combustion gas and the unignited propellant surface on flame-spreading and the rate of pressure increase. The higher the

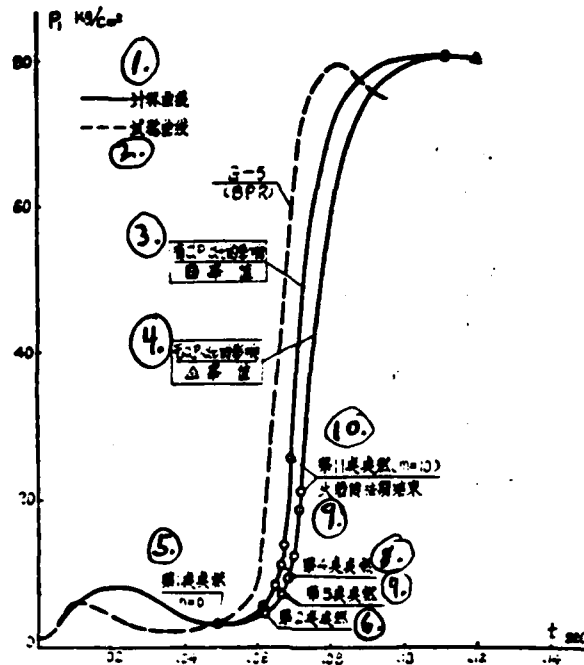


Figure 3. Comparison of computed p-t curves with experimental p-t curve

1--computed curves; 2--experimental curve; 3--effect of dp/dt taken into account; \square --peak value; 4--effect of dp/dt not taken into account; Δ --peak value; 5--first point ignited; 6--second point ignited; 7--third point ignited; 8--fourth point ignited; 9--end of the flame-spreading stage; 10--eleventh point ignited ($m=10$)

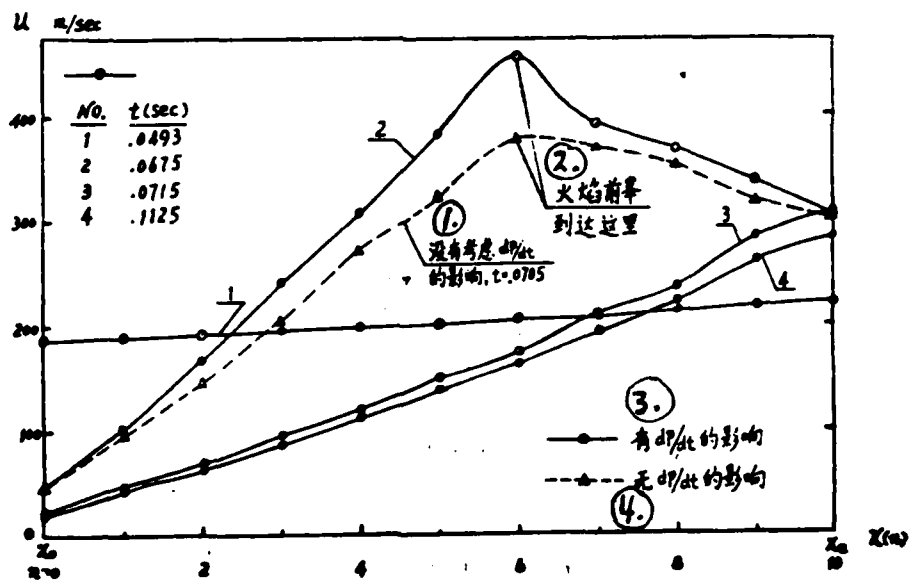


Figure 4. Distribution of velocity along the passage at various moments

1--effect of dp/dt is not taken into account. $t=0.0705$; 2--flame front has reached this point; 3--effect of dp/dt taken into account; 4--effect of dp/dt not taken into account

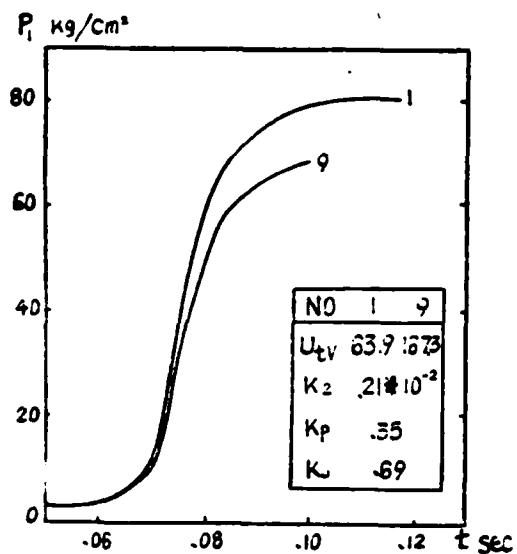


Figure 5. Effect of erosive property of propellant on the starting transient process

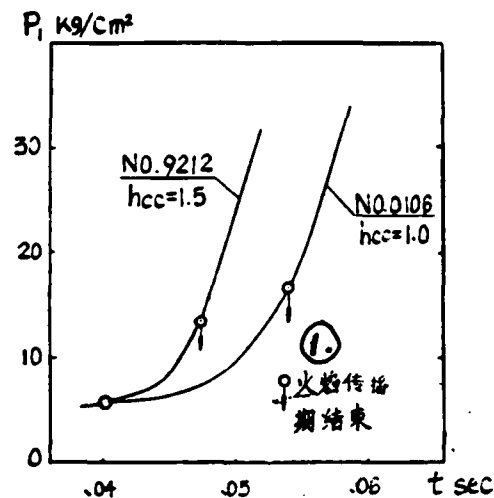


Figure 6. Effect of heat exchange coefficient on flame-spreading 1--end of flame-spreading stage

rate at which energy is acquired by the propellant, the faster the flame-spreading, and the greater the rate of pressure increase. Hence, simulated tests of the starting transient process should also include a simulation of the mode of flame-ejection of the igniter, rate of mass flow, combustion properties of the fuel in the igniter, etc.

REFERENCES

- [1] Kuo, K. K., Vichnevsky, R., and Summerfield, M., "Theory of Flame Front Propagation in Porous Propellant Charges under Confinement", AIAA J. Vol. 11, No. 4, April 1973, pp. 444-451.
- [2] Peretz, A., Kuo, K. K., Caveny, L. H., and Summerfield, M., "Starting Transient of Solid Propellant Rocket Motors with High Internal Gas Velocities", AIAA J., Vol. 11, No. 12, PP. 1719-1727, Dec. 1973.
- [3] Razdan, M. K. and Kuo, K. K., "Measurements and Model Validation for Composite Propellants Burning under Cross Flow of Gases", AIAA J. Vol. 18, No. 6, June 1980, pp. 669.
- [4] Paul, B. E., Lovine, R. L. and Fong, L. Y., "A Ballistic Explanation of the Ignition Pressure Peak", AIAA Preprint 64-121.

END

FILMED

4-84

DTIC